Indian Journal of Geo-Marine Sciences
Vol. 45(8), August 2016, pp. 1010-1016

Tidal Constituents in the Persian Gulf, Gulf of Oman and Arabian Sea: a Numerical Study

P. Akbari[1]*, M. Sadrinasab[2] , V. Chegini[3] , M. Siadatmousavi[4]
1- Khorramshar University of Marine Science and Technolgy, Khorramshar, Iran
2- University of Tehran, Tehran, Iran
3- Iranian National Institute for Oceanography and Atmospheric Science, Tehran, Iran
4- Iran University of Science and Technology, Tehran, Iran
*[E-mail: pakbari91@yahoo.com]

Received 03 July 2015; revised 02 February 2016

In this study, a three-dimensional coastal ocean model (FVCOM) is used in barotropic mode to simulate tidal amplitudes in the Persian Gulf, Gulf of Oman and Arabian Sea. Finite volume method is applied for solving hydrodynamic equations on an unstructured triangular mesh grid. Amplitudes and phases of 8 main tidal constituents are prescribed along the southern open-ocean boundary. To assess the model performance, the model results were compared with observational evidences. Amplitudes of tidal components observed at 9 tidal gauges in the region confirm the results of harmonic analysis performed on model outputs. Hence, it can be concluded that the amplitudes of 8 tidal components are well predicted by the model. Moreover, amphidromic points are accurately predicted from model results for these components. Also M_2 and K_1 are determined respectively as major semi-diurnal and diurnal constituents in entire domain. Finally, the tidal regime is classified by employing the form factor F in this area.

[**Keywords:** Tidal Constituents, Persian Gulf, Gulf of Oman, Arabian Sea]

Introduction

The study of tides as a behavior of the sea is essential in all coastal engineering projects. Harmonic analysis and recognition of main tidal constituents is useful to summarize the tidal information in specific location and to predict the tide heights and tidal currents. Economic, political and industrial aspects of the Persian Gulf depend on its oil and gas resources, thus transforming the region of the Persian Gulf, Strait of Hormuz and Gulf of Oman into one of the most important waterways in the world. Therefore, the tidal information in this area is useful in coastal development projects as well as pollution tracking. Strait of Hormuz (56 km wide) connects the Persian Gulf via the Gulf of Oman with the Arabian Sea. The Persian Gulf is a semi-enclosed basin with an average depth of 35 m. Gulf extends between 24°N and 30°N and 48°E and 56°E and occupies a surface area of ~239000 km^2 [1]. Gulf of Oman has a surface area of ~94000 km^2 and its maximum depth is more than 3000 m. It is located between 22°N and 26°N and 56°E and 60°E[2]. Arabian Sea is situated in the northern boundary of the Indian Ocean and its area exceeds 3×10^6 km^2 and has an average depth of ~2700 m [3]. Although numerous studies have investigated the circulation and different forces impacts on this study area, especially in the Persian Gulf[2,4,5&6], this study focuses on the tidal system and the importance of different tidal components in the Persian Gulf, Gulf of Oman and Arabian Sea. Defant[7] believed the tidal conditions at the Persian Gulf, Strait of Hormuz and Gulf of Oman were different. Because, if these areas are regarded as unified basin, the longitudinal axis of the area must be considered as a canal with two nicks. This would affect the independent tides, where the phase of the tide-generating force would depend upon the longitudinal direction of the basin. Therefore, the tide in the Persian Gulf is a standing wave with different amphidromic points for different constituents, while high water occurs simultaneously over the entire area of the Gulf of Oman[7]. Also, the tides in the Persian Gulf co-oscillate with those in the Strait of Hormuz and the tides in the Gulf of Oman co-oscillate with those in the Arabian Sea (from estimates by Reynolds[8]).

Elahi and Ashrafi[9] analyzed the dynamics of the four major tidal constituents M_2, S_2, K_1 and O_1 in the Persian Gulf using a two dimensional numerical

model. They also classified the area with reference to diurnal and semidiurnal tides using form factor. Najafi[10] modeled tides in the Persian Gulf using dynamic nesting. He found that M_2, S_2, K_1 and O_1 were the major semi-diurnal and diurnal tidal constituents in the Persian Gulf, but he did not explain the tidal conditions of the Gulf of Oman and Arabian Sea. Pous et al.[11] described tidal elevations and velocities in the Persian Gulf and presented the iso-amplitudes and iso-phases of two tidal harmonics (M_2 and K_1) provided by a two dimensional model. In this study, we applied a three dimensional finite volume model over the Persian Gulf, Gulf of Oman and the Arabian Sea. Eight tidal components were forced at the southern boundary, and the model was run in barotropic mode. Harmonic analysis was performed over tidal elevations resulting from the model in nine locations, where tidal gauge recordings existed. Then we skill assessed the model results using the observational data.

Materials and Methods

A three dimensional finite volume coastal ocean model (FVCOM)[12] in spherical coordinates with constant temperature, salinity and density was implemented over a large domain including the Persian Gulf, Gulf of Oman and Arabian Sea (Fig. 1). In this model, the finite volume method was employed to discretize the governing equations on an unstructured triangular mesh grid. The sides of mesh were ~5 km in different directions.

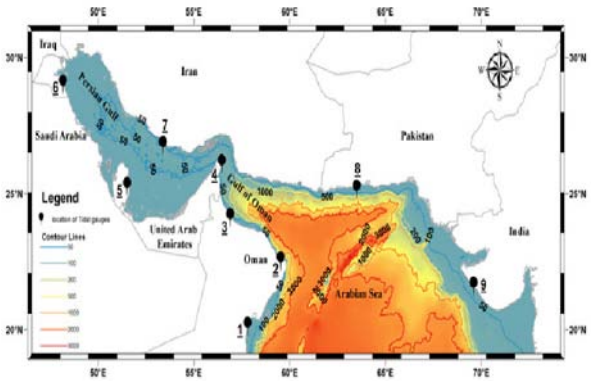

Fig. 1— Bathymetry and geography of the model domain. Black circles indicate the location of tidal gauges used in table1

The model was run in 2D external mode. External time step for this mode was used to solve 2D (vertically-integrated) momentum and continuity equations. The time is bounded through the Courant Fridrich Levy (CFL) stability criterion in the form of

$$\Delta t_E \le \frac{\Delta L}{U + \sqrt{gD}} \qquad (1)$$

Where Δt_E is the time step of external mode, the computational length scale (Δl) is the shortest edge of an individual triangular grid element, U is the magnitude of the horizontal velocity, and D is the local depth[12]. This time step for our study is 20s. Bathymetry data with 1 minute resolution from GEBCO* database[13] was used. The model applied Wet/Dry point treatment method in intertidal zone to provide an accurate simulation of the water transport flooding on to and draining out of these regions. Amplitudes and phases of the four semi-diurnal tidal components S_2, M_2, N_2, K_2 and four diurnal components K_1, P_1, O_1 and Q_1 at each node along the southern open-ocean boundary (considered at 18.5 ° N) were extracted from the Tidal Model Driver (TMD) toolbox [14] and prescribed in the model. Model employed the horizontal diffusion coefficient for momentum, determined by the Smagorinsky eddy parameterization method. According to this method, horizontal diffusion coefficient varies with the model resolution and the gradient of horizontal velocities[15]. Also, the Mellor and Yamada level 2.5 (MY-2.5) turbulent closure model[16] was used for the parameterization of vertical eddy viscosity. Hourly outputs during 200 days are obtained for harmonic analysis. This time period allowed the nonlinear interactions between the eight tidal components to occur, and the amplitude of oscillations reached its final values. Harmonic analysis was used to analysis model output in the entire domain. This semi-empirical method is a mathematical process by which the observed or modeled tide or tidal current at any place is separated into basic harmonic constituents. In our study time step of harmonic analysis is one hour.

Results and Discussion

To assess the model performance, harmonic analysis was applied to the model results at nine stations and the amplitude of eight main components were extracted and compared with the amplitude of tidal gauge data reported by Pous et al.[11]. They selected tidal elevation time-series from tide gauges of the International Hydrographic Office[11].

* General Bathymetric Chart of the Oceans

Amplitudes of the model and observations are listed in Tables 1 and 2. Results of the harmonic analysis on tidal gauge data for Q_1 were not represented by Pous et al.[11].

Table 1— Comparison of modeled (M) and observed (O) values of amplitudes (cm) for four semi-diurnal components

No.	Station	Position	M_2		S_2		N_2		K_2	
			M	O	M	O	M	O	M	O
1	Sirab	20° 10′N 57° 49′E	55.5	57.4	21.0	24.1	14.0	14.0	6.0	6.0
2	Sur	22° 34′N 59° 32′E	58.2	60.0	22.3	23.1	13.8	15.1	6.0	6.1
3	Saham	24° 09′N 56° 54′E	65.6	68.7	25.0	26.1	15.5	17.1	7.1	7.0
4	Ras Dillah	26° 08′N 56° 28′E	69.3	72.1	24.6	27.0	16.8	18.1	6.0	7.0
5	Ad Dawhah	25° 18′N 51° 31′E	33.2	32.0	13.5	11.1	7.9	9.0	5.5	3.1
6	Mina al Ahmadi	29° 04′N 48° 10′E	59.4	63.3	25.1	17.2	24.2	12.0	12.2	5.3
7	Jezirat Lavan	26° 48′N 53° 23′E	31.5	30.1	11.1	12.1	9.4	8.1	3.4	4.1
8	Pansi	25° 12′N 63° 30′E	66.6	72.5	23.4	26.0	14.2	17.3	6.6	7.1
9	Porbandar	21° 38′N 69° 37′E	60.0	65.0	22.5	24.4	13.8	16.1	6.3	7.2
Averaged differences			2.9		2.5		2.6		1.3	

Table 2— Comparison of modeled (M) and observed (O) values of amplitudes (cm) for four diurnal components

No.	Station	Position	K_1		O_1		P_1		Q_1	
			M	O	M	O	M	O	M	O
1	Sirab	20° 10′N 57° 49′E	37.4	39.3	18.5	20.1	10.3	13.2	3.6	–
2	Sur	22° 34′N 59° 32′E	36.5	40.4	17.5	19.0	10.5	13.4	3.7	–
3	Saham	24° 09′N 56° 54′E	35.3	40.4	18.5	22.0	10.0	13.1	3.8	–
4	Ras Dillah	26° 08′N 56° 28′E	28.0	31.1	14.2	19.3	7.2	11.0	4.6	–
5	Ad Dawhah	25° 18′N 51° 31′E	35.5	36.0	28.5	16.1	13.0	10.0	10.0	–
6	Mina al Ahmadi	29° 04′N 48° 10′E	42.0	43.2	39.2	29.3	14.3	14.2	14.7	–
7	Jezirat Lavan	26° 48′N 53° 23′E	26.4	29.5	22.6	15.5	9.4	10.3	7.5	–
8	Pansi	25° 12′N 63° 30′E	35.2	28.0	18.5	21.0	10.0	9.1	3.8	–
9	Porbandar	21° 38′N 69° 37′E	34.1	35.2	16.5	17.0	9.2	10.4	3.5	–
Averaged differences			3.3		4.8		2.1		–	

The most accurate components were M_2 and K_1. The relative differences between the amplitude of the model and observational data are often smaller than 10 percent for aforementioned constituents, and were the same in the Persian Gulf and Arabian Sea. In stations 1, 2, 3, 4, 8 and 9, the importance order of the tidal constituents from high to low were M_2, K_1, S_2, O_1, N_2, P_1, K_2 and Q_1. This arrangement was in agreement with observational evidence in these stations. In station 5, K_1 was the largest component followed by M_2, O_1, S_2, P_1, Q_1, N_2 and K_2 respectively. Again, the observations confirmed this finding. In stations 6 and 7, the first four components were M_2, K_1, O_1 and S_2 respectively, which was consistent with the measurements. But the N_2 component was the next largest constituent after these four components, whereas in measurements in which P_1 was the next important component. This discrepancy between measured and modeled results might be due to the fact that in station 6 measurement data represented close values for P_1 and N_2 components. Also in station 7, P_1 and N_2 components had nearly equal strength according to the model results. Also average values of the differences between model and data amplitudes for seven tidal components are presented in Tables 1 and 2. Average was taken in to account data from all nine stations over entire domain. These differences, which are a few centimeters, show acceptable performance of the model. Iso-amplitude lines for the eight tidal constituents in the study area, provided by the model, are illustrated in Figs. 2 to 9. Due to low accuracy of the model output close to the open boundary, representations of results in this area were eliminated. Figure 2 indicates amplitude of M_2 by contour lines. This tidal component had amplitude of nearly 20 to 50 cm everywhere in the Persian Gulf and reached a maximum of 70-80 cm both at the head of the Gulf and in the Strait of Hormuz. As this figure illustrates, M_2 had two amphidromic points in the Persian Gulf (east of Qatar and in the northwestern part of the Gulf). The exact location of amphidromic points of different constituents in latitude and longitude are listed in Table 3. Amplitude of M_2 had a value of 60 to 70 cm almost everywhere in the Gulf of Oman. Although this amplitude decreased to 50 cm in the

south of the Arabian Sea close to 20° N, in the northeastern part of the Sea it exceeded 60 cm.

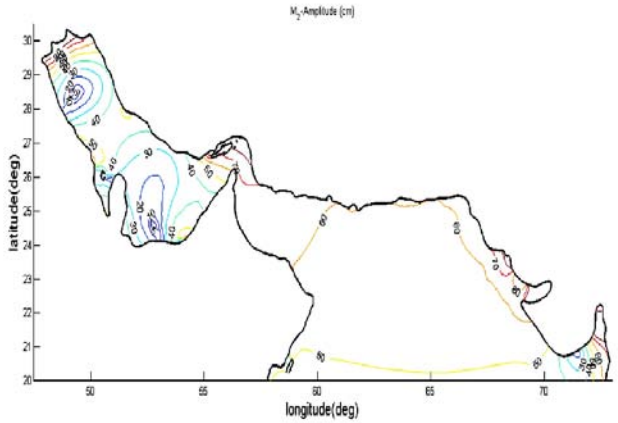

Fig. 2— Iso-amplitude map in cm for tidal component M_2

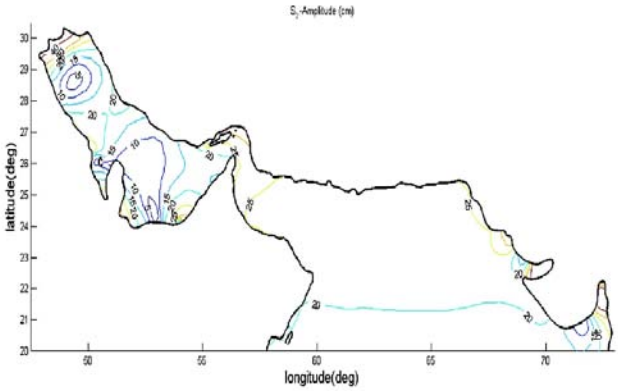

Fig. 3— Iso-amplitude map in cm for tidal component S_2

Amplitude of S_2 is represented in Fig. 3. The amplitude of this component is ~30% of the corresponding amplitude for M_2, and its maxima were located at the head of the Persian Gulf and in the Strait of Hormuz. Two amphidromic points of the S_2 component were located close to the amphidromic points of M_2. Also, descending values for the amplitudes are observed from the Strait to the south of the Arabian Sea. Figure 4 and 5 illustrate the amplitude patterns for N_2 and K_2 constituents respectively. Locations of maxima and amphidromic points of these components were similar to M_2 and S_2. So all of these semi-diurnal components had two amphidromic points in the Persian Gulf, but in the Gulf of Oman and Arabian Sea the tide, as a progressive wave, moved across the sea surface. This finding confirms Defant's theory[7].

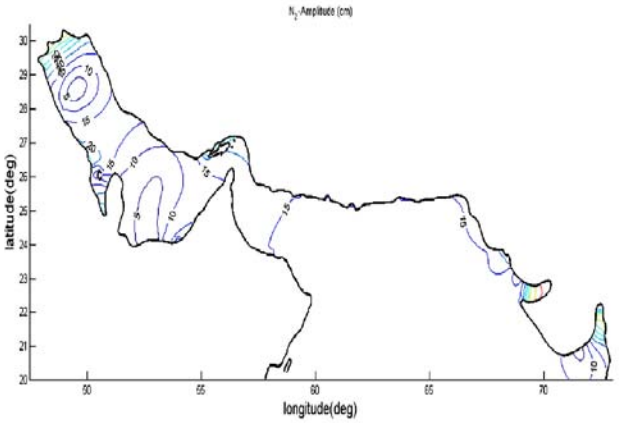

Fig. 4— Iso-amplitude map in cm for tidal component N_2

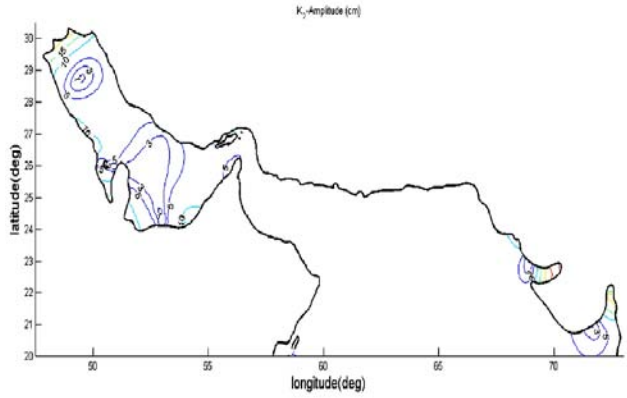

Fig. 5— Iso-amplitude map in cm for tidal component K_2

Amplitude patterns of diurnal components are shown in Figs. 6 to 9, in which K_1 was the most important pattern (see Fig. 6). This constituent represented one amphidromic point in the north of Bahrain and its maximum amplitudes were more than 40 cm at the head of the Persian Gulf. Amplitude in the Strait of Hormuz was 20-30 cm and increased to 35 in the Gulf of Oman. Amplitude of K_1 in the Arabian Sea descended as moved southward and attained values lower than 35 cm close to the southern boundary. The component O_1 was the second most important diurnal component and its amphidromic point and the maximum amplitudes were situated in a location close to the K_1 component (Fig. 7). This amplitude was 15-20 cm in the Strait of Hormuz, Gulf of Oman and Arabian Sea and by decreasing in latitude from the Strait to the southern boundary of the Arabian Sea, amplitude reduction was illustrated as well.

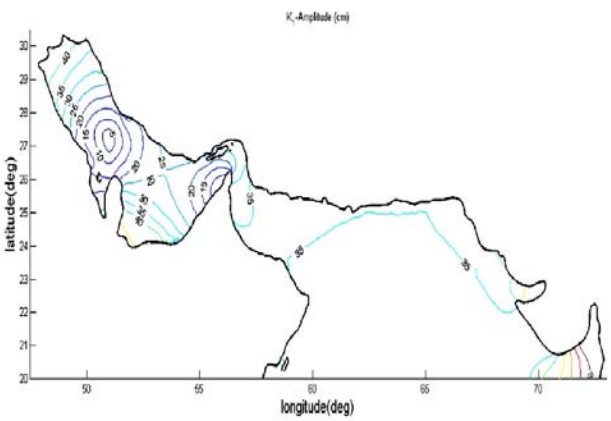

Fig. 6— Iso-amplitude map in cm for tidal component K_1

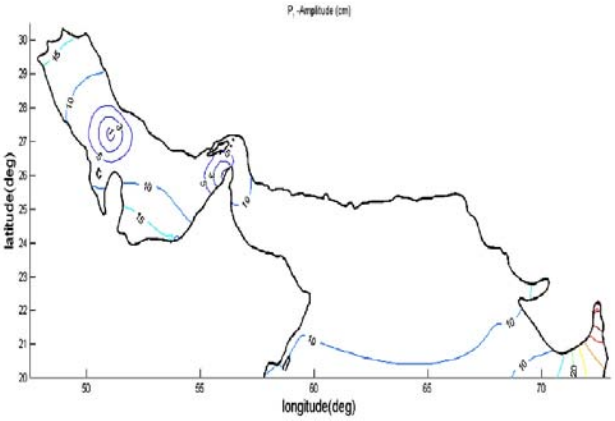

Fig. 8— Iso-amplitude map in cm for tidal component P_1

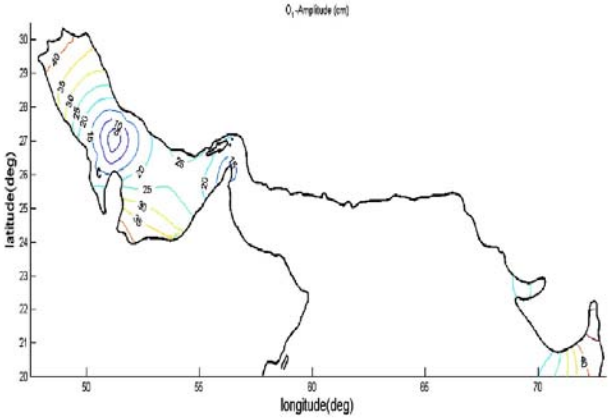

Fig. 7— Iso-amplitude map in cm for tidal component O_1

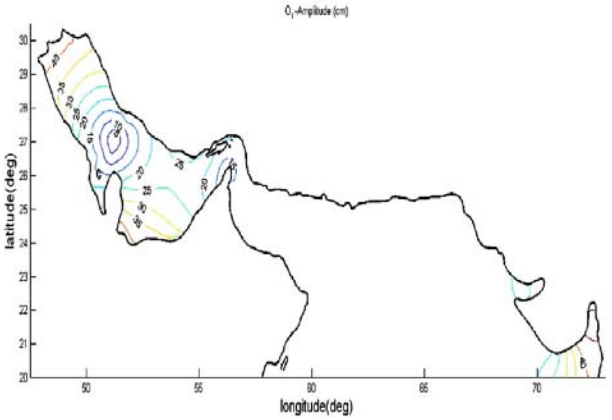

Fig. 9— Iso-amplitude map in cm for tidal component Q_1

Figure 8 and 9 show iso-amplitude lines of P_1 and Q_1 constituents. Maximum amplitudes occurred at the head of the Persian Gulf with a value of 15 cm. Amphidromic point of Q_1 appeared at the north of Qatar in a position east of amphidromic points of the other diurnal components. Amplitude of P_1 was approximately 10 cm almost everywhere in the Gulf of Oman and Arabian Sea and reached to 9 cm close to the southern boundary. Amplitude of Q_1 was lower than 5 cm in the Gulf of Oman and Arabian Sea. Locations of amphidromic points reproduced by the model in this study (see Table 3) were almost similar to the position of these points presented before. However, small displacements were observed among the results of different investigations[9&11]. These displacements were about 0.1 degree in latitude and longitude, probably due to the application of different database for bathymetry data, or different spatial resolutions.

Table 3— Location of Amphidromic Points

Tidal Component	Location of Amphidromic Point
M2	28.4N, 49.3E ; 24.5N, 52.7E
S2	28.6N, 49.4E ; 24.4N, 52.8E
N2	28.6N, 49.5E ; 24.2N, 52.7E
K2	28.7N, 49.5E ; 24.4N, 52.9E
K1	27.1N, 51E
O1	26.9N, 51.2E
P1	27.2N, 51E
Q1	27N, 51.4E

To classify the area according to the nature of the tide, the form factor (F) was applied. It defined as $F= (K_1+O_1) / (M_2+S_2)$; where the symbols of the constituents indicate their respective amplitudes[17]. By using this factor, type of tide was determined as diurnal, semidiurnal and mixed. The F value for each type is presented in Table 4.

Table 4— F values for different types of tide [17]

Value of F	Type of tide
0-0.25	Semidiurnal
0.25-1.5	Mixed, mainly semidiurnal
1.5-3	Mixed, mainly diurnal
>3	Diurnal

Figure 10 shows the value of the form factor in the Persian Gulf, Gulf of Oman and Arabian Sea. According to this figure, in the Persian Gulf - north of Qatar and close to the diurnal amphidromic point – the tide is semidiurnal. This finding is expected because in this region the diurnal component of free surface elevation is close to zero, and semidiurnal components dominate the tidal signal. Inversely, diurnal components dominate close to two semidiurnal amphidromic points, and as a result, the tide is diurnal at those locations. In other places, the tide is mixed. Model shows four types of tide in the Persian Gulf as reported by Pous et al. and Elahi and Ashrafi[9&11]. As Figure 10 indicates and according to Table 4, the tide in the Strait of Hormuz, Gulf of Oman and Arabian Sea was mixed; mainly semidiurnal. Our result for the Strait of Hormuz is in accordance with Pous et al.'s result[11]. However, they did not consider the Gulf of Oman and Arabian Sea in their study area.

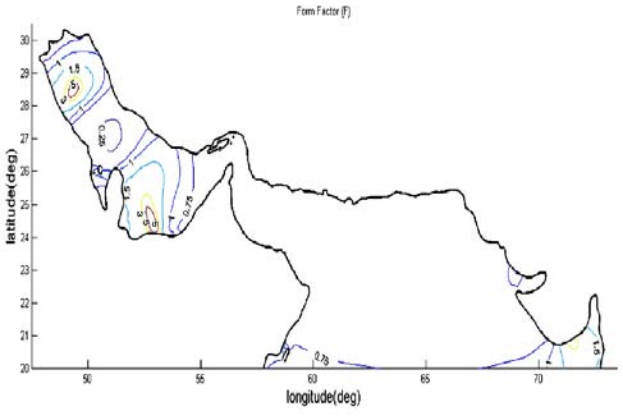

Fig. 10— Map of Form Factor over Persian Gulf, Gulf of Oman and Arabian Sea

Our findings are in good agreement with previous studies[9&11]; however, more tidal components are included in this study in the Persian Gulf and Strait of Hormuz than in those researches.

Conclusion

We have applied a finite volume model, forced by eight tidal components at its southern boundary to study tidal amplitude in an extended domain comprising of the Persian Gulf, Gulf of Oman and Arabian Sea. Model results indicate that the tide in the Persian Gulf is a standing wave with two amphidromic points of semidiurnal components and one amphidromic point of diurnal components. But the tide in the Gulf of Oman and Arabian Sea is a progressive wave which moves across the sea surface. Model identified M_2/K_1 as the most important semidiurnal/diurnal component in the entire domain. In our study area the tide mostly appears as mixed, mainly semidiurnal, except close to the amphidromic points. This tidal information and recognition of main constituents are useful to predict tide heights and tidal currents for engineering applications.

References

1 Emery, K. O., Sediments and water of the Persian Gulf, *AAPG Bull*, 40(1956) 2354-2383.

2 Pous, S., Carton, X. and Lazure, P., Hydrology and Circulation in the Straits of Hormuz and the Gulf of Oman; Results from the GOG99 Experiment. II. Gulf of Oman, *J. Geophys. Res*., 109(2004) 1-263.

3 Chegini V, *Glossary of Coastal Engineering and Physical Oceanography*, (Iranian National Institute for Oceanography, Tehran) 2011, pp. 6085.

4 Chao, S. Y., Kao, T. W. and Al-Hajri, K. R., A numerical investigation of circulation in the Arabian Gulf, *J. Geophys. Res.*, 97(1992) 11219-11236.

5 Kampf, J., Sadrinasab, M., The circulation of the Persian Gulf: a numerical study, *Ocean Sci.*, 2(2006) 27-41.

6 Pous, S., Lazure, P. and Carton, X., A model of the general circulation in the Persian Gulf and in the Strait of Hormuz: Intraseasonal to interannual variability, *Cont. Shelf Res*., 94(2015) 55-70.

7 Defant A, *Physical Oceanography*, (Pergamon Press LTD) Vol. 2, 1960, pp. 571.

8 Reynolds, R. M., Physical oceanography of the Gulf, Strait of Hormuz, and the Gulf of Oman – Results from the Mt Mitchell expedition, *Mar. Pollut. Bull.*, 27(1993) 35-59.

9 Elahi, Kh. Z., Ashrafi, R. A., A two-dimensional depth integrated numerical model for tidal flow in the Arabian Gulf, *Acta Oceanogr. Taiwan.,* 32(1994) 1-15.

10 Najafi, H. S., Modelling tides in the Persian Gulf using dynamic nesting, Ph.D. thesis, University of Adelaide, Adelaide, South Australia, 1997.

11 Pous, S., Carton, X. and Lazure, P., A Process Study of the Tidal Circulation in the Persian Gulf, *Open J. Mar. Sci*., 2(2012) 131-140.

12 Chen, C., Beardsley, R. C., Cowles, G., *An unstructured grid, finite-volume coastal ocean model: FVCOM User Manual*, SMAST/UMASSD Technical Report-06-0602, University of Massachusetts-Dartmouth, New Bedford, 2006.

13 Ioc, I., 2008. BODC, 2003. Centenary Edition of the GEBCO Digital Atlas, published on CD-ROM on behalf of the Intergovernmental Oceanographic Commission and the International Hydrographic Organization as part of the General Bathymetric Chart of the Oceans. British oceanographic data centre, Liverpool.

14 Padman, L., Erofeeva, S., *Tide Model Driver (TMD) Manual*, Earth & Space Research Institute, Seattle, 2005.

15 Smagorinsky, J., General circulation experiments with the primitive equations, I. The basic experiment, *Monthly Weather Review*, 91(1963) 99-164.

16 Mellor, G. L., Yamada, T., Development of a turbulence closure model for geophysical fluid problem, *Rev. Geophys. Space. Phys*, 20(1982) 851-875.

17 Van Rijn L C, *Principles of fluid flow and surface waves in rivers, Estuaries, seas and oceans*, (University of Utrecht, The Netherlands) 1990, pp. 335.